

MICRO-FTIR AND MICRO-RAMAN STUDY OF PAINTS USED BY SAM FRANCIS

FULL PAPER

Michel Bouchard*, Rachel Rivenc, Carrie Menke, Tom Learner

This paper is based on a presentation at the 8th international conference of the Infrared and Raman Users' Group (IRUG) in Vienna, Austria, 26-29 March 2008.

Guest editor:
Prof. Dr. Manfred Schreiner

Getty Conservation Institute, 1200 Getty Center Drive, Suite 700, Los Angeles, CA 90049, USA

corresponding author:
mbouchard@getty.edu

Raman microscopy and Fourier-transform infrared (FTIR) analyses were both utilized in a recent study of the painting materials used by the American artist Sam Francis (1923-94), in particular a collection of sixty-four pots of custom-made, pre-mixed paints that were found in his Santa Monica studio after his death. Although other analytical techniques were also used in this study, this paper reports on the performance of FTIR and Raman microscopy, with a particular emphasis on their relative ability to detect synthetic organic pigments. These pigments are often hard to detect in paint samples due to their very small particle size, and the fact that only minimal quantities are needed in some paint formulation to produce extremely vivid colours. In general, Raman microscopy was found to be more successful in detecting all pigments, both organic and inorganic. Sixteen different organic pigments were identified by Raman microscopy in thirty-five of the paint samples, including those from the azo, phthalocyanine, quinacridone, disazo, diarylide, dioxazine, indanthrone and perinone families. In contrast, FTIR only detected organic pigments successfully in eighteen of the paint samples, and in most of the cases where FTIR failed it was due to the strong and broad absorptions of the fillers. The inorganic pigments identified by Raman included natural and synthetic pigments such as hematite, goethite, magnetite, cobalt phosphate, cobalt titanate, ultramarine, amorphous material such as graphite but also baryte and calcite fillers. FTIR was also effective in detecting fillers, but very few of the inorganic pigments. However, FTIR appeared much better suited to the detection of the binder, primarily an acrylic emulsion, which typically gave very strong and distinctive peaks, compared to the fairly weak and broad peaks visible with Raman microscopy. The two techniques appeared very complementary and the use of both was required to gather a complete understanding of Francis' paints composition.

received: 04/06/2008
accepted: 24/03/2009

key words:
Raman, FTIR, modern, organic,
inorganic, paint



Figure 1: Paint pots and painting materials left in Sam Francis' studio in Santa Monica.

1 Introduction

Sam Francis (1923-1994) was one of the most influential American painters of the 20th century. Francis painted in several media throughout his life, but he made frequent use of acrylic emulsion after 1970. From discussions with Dan Citron - his studio assistant and paint maker for many years - it was learned that Francis used both commercially available paints as well as custom-made formulations prepared by Citron that often included a broad range of pigments that were not commonly found in artist's paints. Francis lived primarily in California and it was there, in his studio in Santa Monica, that sixty-four pre-mixed containers of paints were found after his death (Figure 1).

As part of an ongoing study into the materials used by Francis, the paint from each of these containers was investigated, in addition to samples from an archive of discarded paint-outs and long paint brush handles and a number of his paintings. This paper focuses on assessing the possibilities, limitations and complementarities of Fourier Transform InfraRed (FTIR) spectroscopy and Raman microscopy in the analysis of these paint samples. A number of other analytical techniques were also used for this project, including in particular Scanning Electron Microscopy-Energy Dispersive X-ray analysis (SEM-EDX) for the inorganic components, and Direct Temperature-resolved Mass Spectrometry (DTMS) for organic synthetic pigments - the results of which are published elsewhere.¹ However, it was found that a combination of FTIR and Raman microscopy enabled the vast majority of pigments (both inor-

ganic and organic) and binders to be identified in all the paint samples studied.

FTIR is often one of the first technique to be used in the analysis of paint materials, and it has been shown to be a highly effective tool for identifying many of the components found in modern paints.^{2,3} However, complications can quickly arise in the interpretation of spectra when peaks from the various components overlap. One group of materials that has proved particularly difficult to detect has been synthetic organic pigments, primarily due to the fact that they tend to exhibit extremely high tinting strengths, and as a result are often only added in very low concentrations to a paint formulation. In addition, their peaks can become masked behind the very strong and broad absorptions typically seen in the spectra of inorganic fillers and extenders (e.g. CaCO₃). In recent years, some progress has been made with modifying sample preparation techniques to improve the relative strength of the characteristic peaks from organic pigments by e.g. removing the extenders with acid.⁴ However, this process remains fairly time-consuming, and there are a number of pigments and fillers that do not appear to respond to this approach. FTIR does remain a viable detection method for organic pigments, however, as most pure organic synthetic pigments give spectra with very diagnostic fingerprint regions.^{3,5}

FTIR microscopy requires a reasonably small sample size, and in some instances can even be seen as non-invasive if an Attenuated Total Reflectance (ATR) mode is used in which an area of 10-20 μm² is typically measured.⁶ Although much larger than the area necessary for Raman analysis, this is not necessarily a disadvantage as a larger area is more representative of the sample.

Raman microscopy has already proved its potential for the identification of inorganic pigments in works of art.⁷⁻¹² The crystallinity and high symmetry of many mineral pigments facilitates their study by Raman microscopy. In addition, Raman microscopy permits the differentiation between polymorph minerals (e.g. hematite from maghemite). It is often viewed as a "non-invasive" technique¹, in addition the recent development of portable, hand-held Raman devices clearly holds much promise for a totally non-invasive application of Raman spectroscopy, but as yet the instruments do not deliver the same quality spectra as lab-

1. As a counterpart to non-invasive techniques where no sampling tool is involved, "invasive techniques" (in which one can distinguish two sub-criterion, "destructive" and "non-destructive") require the use of a scalpel. A "non-destructive" technique does require sampling, but preserves the sample with all the information that it could still provide after analyses, while samples used in "destructive techniques" are altered either by coating, flattening or they are consumed.

based instruments. One of the great advantages of Raman microscopy is its confocal capability that allows analysis to be performed through a glass sheet or a varnish layer without the need to take a sample, or remove a varnish or even take a glazed painting out of its frame. The spot size for analysis is very small, typically around 1-2 μm in diameter.

The main limitation of Raman microscopy is strong fluorescence that can be sometimes associated with the organic binding media and which can overwhelm the Raman vibrational bands originating from the pigment. Fluorescence may also arise from impurities or from the sample itself. If impurities are the origin of a fluorescent signal, it is sometimes possible to reduce the fluorescence by irradiating for a period of time before collecting a spectrum. Otherwise, it is often a matter of experimentation to determine the best balance between reducing fluorescence and maximizing the Raman signal. Software is often used to apply a baseline correction to remove the large fluorescent “hump” overlaying the spectrum, or first or second derivatives may be employed, as Raman bands are much sharper than fluorescence bands. Raman microscopy can also sometimes be difficult to apply to opaque or dark materials, where strong absorption of the laser beam may lead to possible local burning of the particle.¹³ The relative Raman scattering of different compounds within a mixture can also lead to a misinterpretation of the mixture composition if sufficient care is not used by the operator.

One further difficulty with Raman microscopy, especially in the case of synthetic organic pigments, is the lack of centralized databases as well as of efficient matching softwares. While inorganic Raman databases recently became widespread in published journals^{e.g. 14,15} or online,^{e.g. 16-18} readily available Raman databases of organic material are still lacking or rare.^{e.g. 11,19}

2 Experimental

2.1 Samples

Samples of each of the sixty-four paints were applied to glass microscope slides and allowed to dry. The pots were numbered sequentially SF#1 to SF#64, and this nomenclature was kept for the project. The archive material came from the Getty Research Institute collection, and the paintings investigated were owned by the Sam Francis Foundation or Jonathan Novak Contemporary Art in Los Angeles.

2.2 FTIR

The FTIR spectra of the reference studio paints were collected on a Thermo Nicolet Avatar 360 FTIR spectrometer, using a Smart Orbit ATR accessory and a germanium crystal. The spectra are the sum of 128 scans at a resolution of 4 cm^{-1} . Samples from the archive material and paintings - as well as some samples from the paints pots - were analyzed in transmittance mode using a 15X Refflachromat objective attached to a Nic-Plan (Thermo Electron Corp.) FTIR microscope, and purged with dry air. A few micrograms from each sample were placed on a one-millimeter thick diamond window and flattened using a metal roller to form translucent samples. The samples were analyzed individually using a transmitted infrared beam apertured to 200 x 200 micrometers. The spectra obtained (with both FTIR and Raman) were interpreted and compared to published, commercial or personal spectral databases. All FTIR spectra are shown in transmittance mode, although the Y axis is not shown in the figures when spectra are stacked.

2.3 Raman Micro-spectroscopy

The Raman instrument employed was a Renishaw *InVia* Raman micro-spectrometer coupled to a Leica DMLM microscope. After wavenumber calibration using the silicon peak at $520.5 \pm 1 \text{ cm}^{-1}$, the painted glass slides were simply placed under the microscope objective (20x/0.4 and L50x/0.5) for observation and analysis. The Raman spectra were acquired under the following operational conditions: 785 nm RL 785 HPNIR laser excitation (neutral density filters used to keep laser power at $\sim 10 \text{ mW}$ on the sample to avoid degradation; 1200 l/mm grating, Peltier cooled CCD array detector; integration time 60-150 s and 2-5 accumulations over the spectral range 100-3500 cm^{-1} . For routine analysis, $\pm 2 \text{ cm}^{-1}$ is considered to be the accuracy when comparing spectra from different samples, on different days, or from different instruments. The spectra presented in figures 2-14 are baseline corrected (subtraction of multipoint fit to baseline).

3 Results and Discussion

Table 1 lists the sixty-four different paints from the Francis studio, along with the identifications made for both pigments and media from their FTIR and Raman spectra. Table 1a gives the results for those paints in which organic pigments were detected, and Table 1b those that contain inorganic pigments. In all tables the notations (vw), (w), (s) and (sh) correspond respectively to bands of

Paint ID and color		Raman (pigments)	FTIR (medium & pigments)	
SF01	orange	PO43	EA/MMA	PO43
SF02	yellow	Diazo, e.g. PY12, 126, 127	EA/MMA	no match
SF03	orange-yellow	PO72	EA/MMA	no match
SF04	red	PR170	EA/MMA	PR170
SF05	deep red	PR7	EA/MMA	PR7
SF06	bright yellow	PY3	EA/MMA	PY3
SF08	purple	PV23	EA/MMA	PV23
SF09	purple	PV23	EA/MMA	no match
SF12	red	PR188	EA/MMA	PR188
SF13	dark green	PG7	EA/MMA	PG7
SF14	dark green	PG7	EA/MMA	PG7
SF17	orange-yellow	PY83	EA/MMA	PY83
SF18	dark blue	PB15-1, 2	EA/MMA	PB15
SF19	brown	PO49	EA/MMA	PO49
SF20	bright orange	PO43	EA/MMA	PO43
SF22	purple	PV23	EA/MMA	PV23
SF23	red	PO43	--	--
SF24	orange-yellow	PY83	EA/MMA	PY83
SF29	deep orange	PO5	EA/MMA	PO5
SF31	translucent green	PG36	EA/MMA	no match
SF32	deep red	PR42	--	--
SF34	lilac	PV23	EA/MMA	no match
SF35	green	PG36	EA/MMA	no match
SF42	pale blue-green	Phthalo blue+ Phthalo green + rutile	EA/MMA	no match
SF46	lilac	PV23 + rutile	EA/MMA	no match
SF48	dark green	PG36 + C	EA/MMA	no match
SF49	black	C	EA/MMA	no match
SF51	dark blue	PB60	EA/MMA	PB60
SF52	olive green	PY12	EA/MMA	no match
SF53	pink	PR112	EA/MMA	no match
SF58	blue-green	PG36+ possible PG7	EA/MMA	no match
SF59	red	PR42	--	--
SF60	dark green	PB15:3, 4	EA/MMA	possibly PB15
SF62	bright green	PG36	EA/MMA	no match
SF63	dark brown-violet	PV23	--	PV23

* Artistic names, color index labels and mineral names are all listed in this table.

Table 1a: Listing and composition of the different organic pigments found in the pots of paint from Sam Francis.

very weak, weak, and strong relative intensities and shoulder bands. Generally the mineral and organic composition of all paints were successfully characterized by a combination of Raman microscopy and FTIR, although Raman showed

Paint ID and color		Raman (pigments)	FTIR (medium & pigments)	
SF07	turquoise	Cobalt teal (titanate) PG50	EA/MMA	Ti white
SF10	dark blue	Ultramarine	EA/MMA	Ultramarine?
SF11	bright blue	Ultramarine	EA/MMA	Ultramarine?
SF15	red	Barite	EA/MMA	Barite
SF16	red-violet	Cobalt violet light (NH ₄ CoPO ₄ ·H ₂ O)	EA/MMA	no match
SF21	black	Magnetite	EA/MMA	no match
SF25	honey	Rutile	EA/MMA	no match
SF26	powdery blue	Calcite+ Ultramarine	EA/MMA	Chalk ultramarine
SF27	green	Cobalt green-based	EA/MMA	Ti white
SF28	dark brown	Hematite+ possibly manganese oxide	EA/MMA	no match
SF33	black	Ultramarine + Carbon	EA/MMA	Possibly ultramarine
SF36	pale yellow	Rutile	EA/MMA	Ti white
SF37	deep turquoise	Cobalt green-based	EA/MMA	no match
SF39	terracotta	Hematite	EA/MMA	no match
SF40	yellow-brown	Goethite	EA/MMA	Fe oxide?
SF41	brown	Hematite	EA/MMA	Fe oxide?
SF43	blue	Cobalt blue	EA/MMA	no match
SF44	pink-violet	Cobalt violet light (LiCoPO ₄)	EA/MMA	no match
SF45	red-brown	Hematite	EA/MMA	Possibly Fe oxide
SF47	dark blue	Ultramarine+ C	EA/MMA	no match
SF50	white	Rutile + Calcite	--	no match
SF54	white	Rutile	EA/MMA	no match
SF55	green	Cobalt green	EA/MMA	no match
SF56	orange-brown	Hematite	EA/MMA	no match
SF57	black	Manganese oxide (poss β-MnO ₂)	EA/MMA	no match
SF61	dark brown	Goethite + Carbon	EA/MMA	no match
SF64	purple-blue	Ultramarine, traces of organic pigment	EA/MMA	Ultramarine

* Artistic names, color index labels and mineral names are all listed in this table.

Table 1b: Listing and composition of the different inorganic pigments found in the pots of paint from Sam Francis.

distinct advantages over FTIR when it came to identifying the full range of organic pigments used in these samples.

3.1 The Organic Pigments

Sixteen different organic pigments (in addition to carbon black pigment) were detected in thirty-five of the pre-mixed paints and could be classified according to their structures into five main chemical groups: monoazo, disazo, quinacridone, dioxazine and phthalocyanine.²⁰ Figure 2 shows a selected Raman spectrum for each of these

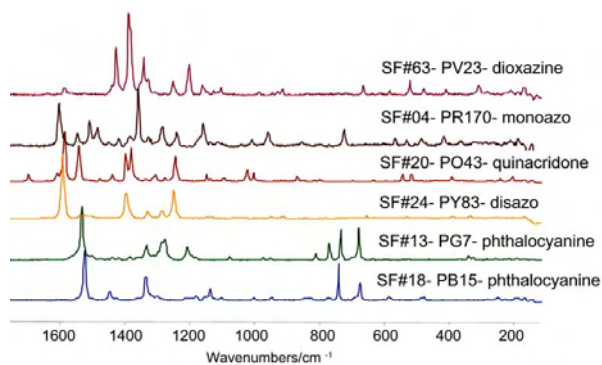


Figure 2: Raman spectra of the different groups of synthetic organic pigments.

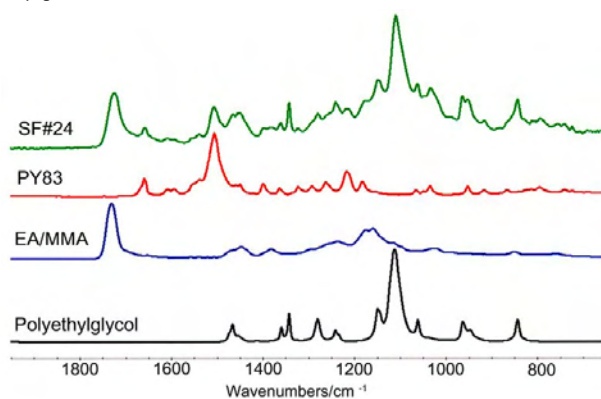


Figure 3: FTIR spectra (transmission) of paint sample SF24, reference spectra of pigment yellow PY83, Winsor and Newton EA/MMA binding medium and the polyethylglycol surfactant.

groups (with two examples of paints containing phthalocyanine pigments). In all these cases Raman microscopy gave very distinctive spectra that closely matched the reference spectra of the relevant dried pigments, with no masking from any overlapping peaks from the binder or fillers, and they could easily be differentiated from each other.

In these spectra the low wavenumber region (0-1000 cm^{-1}) corresponds mainly to the skeletal vibration and ring deformation of the molecules, while the high wavenumber region (1000-1800 cm^{-1}) is more attributable to C-H deformation, C=C aromatic, C=C, C-C, N=N and C-N stretching vibrations.²¹ Some of the spectral features are not specific to a particular pigment but are characteristic of the pigment class. For example, the Raman feature located at c.1400 cm^{-1} is particular to the azo N=N symmetric stretching vibrations of diazo molecules²² as seen in the spectrum of PY83.

Although the azo N=N stretching mode produces a very intense Raman band, it is absent or very weak in IR spectra due to its high symmetry.²¹ However, other features specific to diarylide pigments permit their identification, such as the: (i) absence of carbonyl vibration and (ii) presence of an amide stretching band at $\sim 1659 \text{ cm}^{-1}$ (Figure 3).

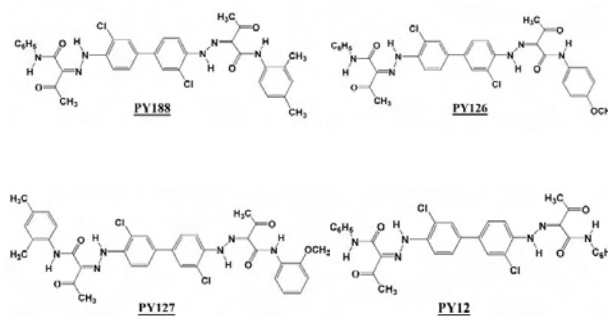


Figure 4: Molecular structure of the different disazo pigments: PY188, PY126, PY127 and PY12.

The Raman band located at c.1600 cm^{-1} (PY83, Figure 2) is specific to the aromatic ring vibration while the IR band located at 1506 cm^{-1} (PY83, Figure 3) is assigned to the aromatic C=C skeletal ring breathing.^{5,23} In addition to IR features specific to their class, which have been described by Lomax and co-workers,⁵ most organic synthetic pigments exhibit fairly distinctive patterns in the fingerprint region of the IR spectrum. For example, Figure 3 shows the IR spectrum of paint sample SF24, together with the reference spectrum of PY83, as well as reference spectra for a pEA/MMA (ethylacrylate/methylmethacrylate) binder and a polyethylglycol surfactant. It is interesting to note that when FTIR is used in the ATR mode, the presence of this class of non-ionic surfactant, which has migrated to the surface from the bulk film, is often a strong feature of dried acrylic emulsion paints.²⁴ Although the IR spectrum of paint sample SF24 is dominated by features from the organic binder and surfactant, the peaks from the pigment PY83 are still adequately visible in the fingerprint region, and it was possible to readily identify it with a library search.

Differentiation of organic pigments with similar chemical structures can, however, be a challenge with both FTIR and Raman microscopy. Take, for example, the four disazo pigments shown in Figure 4.

The Raman and IR spectra of paint sample SF02 are shown in Figures 5 and 6 respectively, along with the spectra of four different reference disazo pigments: PY12 (Sun Chemical), PY126 (Clariant), PY127 (Lansco) and PY188 (Ciba):

Although it is practically impossible to distinguish these pigments by comparing their Raman spectra (due to the high similarity of their structures, see Figure 4), Raman microscopy permits to characterize the pigment of paint sample SF02 as pertaining to the disazo group thanks to specific Raman bands, such as the N=N symmetric stretching band at 1399 cm^{-1} . The full listing of Raman

SF02	PY12	PY126	PY127	PY188
	123	123	123	
	171 (sh)	171 (sh)	171 (sh)	171 (w)
	182	182	182	
	203	203	203	
	284 (w)	284 (w)	284 (w)	274 (vw)
332	330	330	330	
363	365	365	365	363 (w)
	399 (vw)	399 (vw)	399 (vw)	399 (w)
	408 (vw)	408 (vw)	408 (vw)	
	419 (vw)	419 (vw)	419 (vw)	419 (vw)
	439 (w)	439 (w)	439 (w)	439 (w)
	448 (w)	448 (w)	448 (w)	444 (vw)
	471 (vw)	471 (vw)	471 (vw)	492 (vw)
512 (w)	515	515	515	
				541 (vw)
	578 (vw)	578 (vw)		
	613	613	613	
	623 (w)	623 (w)	623 (w)	623 (w)
661	661 (s)	661 (s)	661 (s)	659 (s)
	710 (vw)	710 (vw)	710 (vw)	710 (vw)
	717 (vw)	717 (vw)	717 (vw)	721 (vw)
	785 (vw)	785 (vw)	785 (vw)	
813 (w)	819 (vw)	819 (vw)	819 (vw)	
855 *	871 (w)	871 (w)	871 (w)	
915 (vw)	917	917	917	912 (vw)
				938 (w)
951 (vw)	953	953	953	953
1000 (vw)	1001 (w)	1001 (w)	1001 (w)	1001 (vw)
1048 (vw)	1050 (w)	1050 (w)	1050 (w)	1050 (w)
	1065 (w)	1065 (w)	1065 (w)	1066 (w)
1140 (w)	1141 (w)	1141 (w)	1141 (w)	1147 (w)
	1179 (vw)	1179 (vw)	1179 (vw)	
1184 (vw)	1187 (vw)	1187 (vw)	1187 (vw)	1187 (vw)
1253 (sh)	1253 (s)		1253 (s)	1254 (sh)
1255 (s)	1258 (s)	1256 (s)	1258 (s)	1258 (s)
	1267 (sh, w)	1267 (sh, w)	1267 (sh, w)	1267 (sh, w)
1293	1295	1294	1295	1290
1319 (w)	1321 (w)	1321 (w)	1321 (w)	1317 (w)
1399 (s)	1401 (s)	1401 (s)	1401 (s)	1401 (s)
1449	1450 (w)	1450 (w)	1450 (w)	1448 (w)
	1493 (vw)	1493 (w)	1493 (vw)	1493 (vw)
1518 (w)	1520 (w)	1520 (w)	1520 (w)	1525 (w)
1597 (s)	1599 (s)	1599 (s)	1599 (s)	1600 (s)
1664(w)	1663 (w)	1663 (w)	1663 (w)	1633 (w)

Table 2: Raman bands (wavenumbers/cm⁻¹) of the different disazo pigments (PY12, PY126, PY127 and PY188) in comparison with the bands of yellow paint sample SF2. (*This band is attributed to the binder (pEA/MMA or pBA/MMA)).

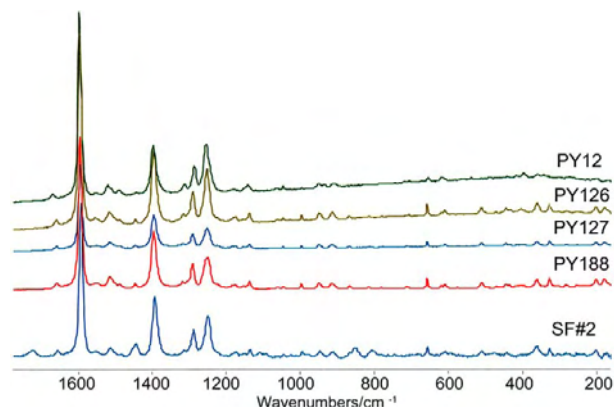


Figure 5: Raman spectra of different disazo pigments in comparison with the spectra of yellow paint sample SF2.

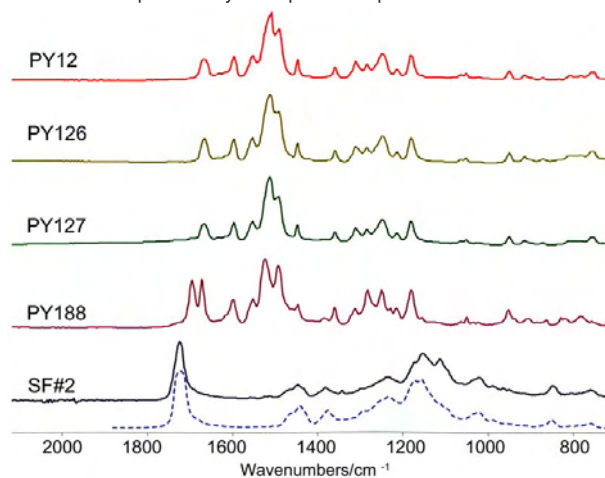


Figure 6: FTIR spectra (transmission) of different disazo pigments in comparison with the spectra of yellow paint sample SF2, the spectrum of the medium EA/MMA is shown by the dashed line.

bands of each of the four pigments, along with those visible from SF02 are given in Table 2. While FTIR analyses seems to rule out the presence of PY188, further identification of the pigment could not be achieved because of the overwhelming presence of features from the binder (showed by the dashed line in Figure 6). Additional DTMS analyses¹ also ruled out PY12, as well as PY188 but could not discriminate between PY126 and PY127.

3.2 Inorganic Pigments

Eleven inorganic pigments or extenders were detected in the different paints collected from Sam Francis' studio. Goethite (α -FeOOH) and hematite (α -Fe₂O₃) were for instance easily distinguished by their Raman spectra, in two paints rather close in color, respectively SF40 (yellow brown) and SF41 (brown). The characteristic Raman features^{15,25} of goethite are located at 92, 247, 300, 387, 485, 552 cm⁻¹, whereas the seven characteristic bands of hematite appear at 224, 245, 291, 299 (shoulder), 411, 498 and 611 cm⁻¹ (Figure 7).

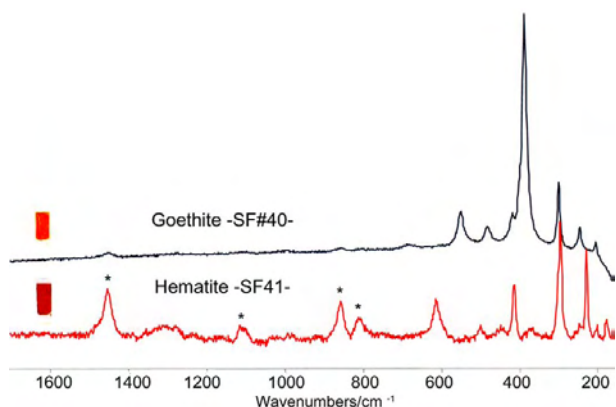


Figure 7: Raman spectra of goethite and hematite clearly distinguished in two different paint samples SF40 and SF41, *correspond to bands of the binder.

Cobalt chrome green		Cobalt blue		Cobalt teal	
SF55 & 37	Ref ¹⁵	SF43	Ref ^{27,15}	SF7	Ref ²⁸
		179 (w)		256	261
190	195	204	201	348	355
		412	412	402	401
515 (s)	513 (s)	516 (s)	512 (s)	526	523
690 (s)	685 (s)			702 (s)	710

Table 3a: Raman bands (wavenumbers/cm⁻¹) of the different cobalt-based pigments identified in the pots of paint and compared to literature.

Cobalt violet I		Cobalt violet II	
SF16	[CoNH ₄ PO ₄ ·H ₂ O]	SF44	[LiCoPO ₄]
	190 (w)	207 (vw)	207 (w)
	223 (w)		254 (w)
	263 (w)		588 (w)
	432 (vw)	632	633 (w)
	558 (w)		
939 (s)	939 (s)	949 (s)	949 (s)
		984 (vw)	986 (vw)
		1074 (vw)	1072 (w)
			1261 (vw)
			1381 (w)

Table 3b: Raman bands (wavenumbers/cm⁻¹) of the two different sorts of cobalt phosphate-based pigments identified in the paint samples SF16 and SF44 along with the two reference pigments confirmed by XRD.

Raman microscopy proved particularly efficient in discriminating between different types of cobalt-based pigments. Samples SF7, SF16, SF37, SF43, SF44 and SF55 (Table 3a and 3b) all contain cobalt-based pigments (Figure 8) but Raman microscopy was able to distinguish between *cobalt chrome green* (cobalt chromite spinel, PG26), *cobalt blue* (cobalt aluminate) *cobalt teal* (cobalt titanate, PG50), and two different types of *cobalt violet light*. The latter were both thought to be

cobalt ammonium phosphates but presented a significant shift (~10 cm⁻¹) at the wavenumber position of the (PO₄)³⁻ symmetric stretching Raman vibrations occurring at ~940 cm⁻¹. In fact it required X-ray diffraction to show that the pigment present in SF16 is a cobalt ammonium phosphate hydrate²⁶ [CoNH₄PO₄·H₂O] while the pigment present in SF44 is a lithium cobalt phosphate²⁷ [LiCoPO₄].

Another example of the possibility for analyzing inorganic paint components with Raman microscopy is the clear distinction between different black pigments. Black and opaque pigments are very sensitive to heat from laser absorption which can lead to local modifications of the mineral composition. As shown in Figure 9, magnetite (Fe₃O₄), graphite (or *carbon black* pigment) and a manganese-based pigment were easily identified with Raman. Magnetite has four predicted Raman bands³⁰ located at 193, 306, 538 and 668 cm⁻¹. Graphite is distinguished by its *sp*² (ca. 1582 cm⁻¹) and the *sp*³ (ca. 1330 cm⁻¹) Raman bands,³¹ while the manganese-based pigment (possibly β-MnO₂) is suggested by the presence of the Mn-O lattice Raman vibration³² at 580 cm⁻¹. The good resolution of the spectra and lack of local heating on the sample are probably due to the pigments being

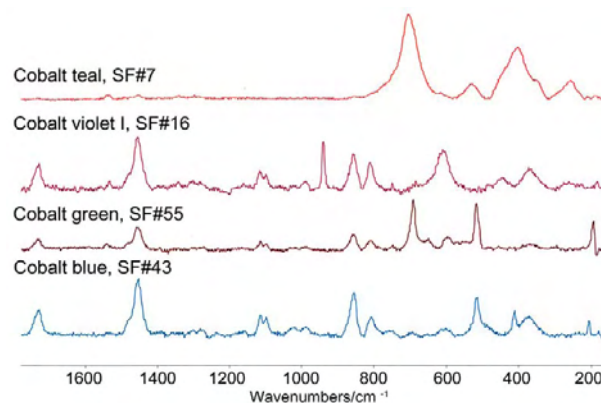


Figure 8: Raman spectra of the different kinds of cobalt-based material identified in the pots of paints.

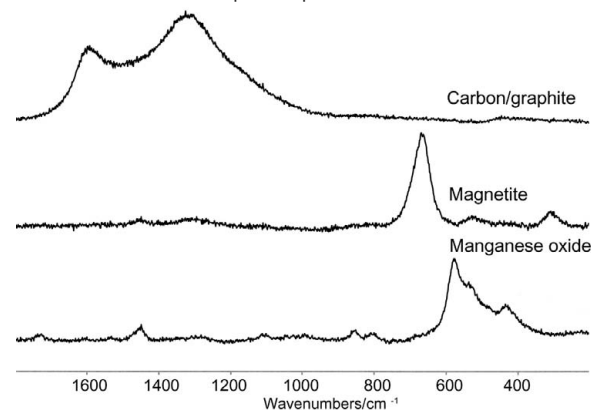


Figure 9: Raman spectra of the three different black pigments used in Sam Francis' paints.

embedded in an acrylic matrix and applied to a glass sheet, which will quickly reduce any local heating of the mineral grains by thermal diffusion effects.

FTIR is not as well-suited as Raman microscopy for the characterization of inorganic compounds particularly in complex mixtures. A significant limitation with FTIR in this study was the cut-off of the detector used which does not record absorptions below 650 cm^{-1} , a region where many inorganic compounds have diagnostic absorptions. Another major interference was encountered when paints contained extenders: sulfates, silicates or carbonate-based minerals produce very broad infrared bands and overlap the fingerprint region of any other inorganic (or indeed organic) contribution from the mixture. FTIR investigation on the different paints permitted the identification of a number of inorganic components, pigment or filler, but rarely of the whole paint system. For example goethite was identified in paint sample SF40, with IR bands^{33,34} occurring at 788 or 898 cm^{-1} . Another example of identification of inorganic material by using FTIR is illustrated by sample SF26 where calcite ($\sim 880\text{ cm}^{-1}$ ν_2 , out-of-plane bend- and $\sim 1400\text{-}1500\text{ cm}^{-1}$ ν_3 , asymmetric stretch-)³⁵ and ultramarine pigment (1019 cm^{-1} , Si-O stretching) were both detected (Figure 10).³⁶

However, Raman microscopy also has limits in its ability to detect inorganic pigments. The Raman spectra in Figure 11 illustrate how the presence of a low scattering compound in a paint can affect the analyses and interpretation: paint SF25 (beige color) shows a Raman spectrum consistent with a poly (ethacrylate / methylmethacrylate) [pEA/MMA] copolymer. No other bands other than those attributable to the medium could be detected.

For comparison, Figure 11 also shows the Raman spectrum from poly (butylacrylate / methylmethacrylate) [pBA/MMA], the other acrylic copolymer that is commonly used as a binder in acrylic emulsion paint formulations. Raman microscopy was not able to differentiate between these two classes of acrylic binder. The two bands located at 1099 and 1116 cm^{-1} appear to be specific to pEA/MMA but the overall very weak scattering cross-section of the organic binding medium doesn't allow these bands to be observed in most *in-situ* case studies. Although binding media are not the primary focus of this paper, it should be mentioned that the two acrylic co-polymers, pEA/MMA and pBA/MMA were both readily identified by FTIR in these paints. The FTIR spectra of these two copolymers have been published else-

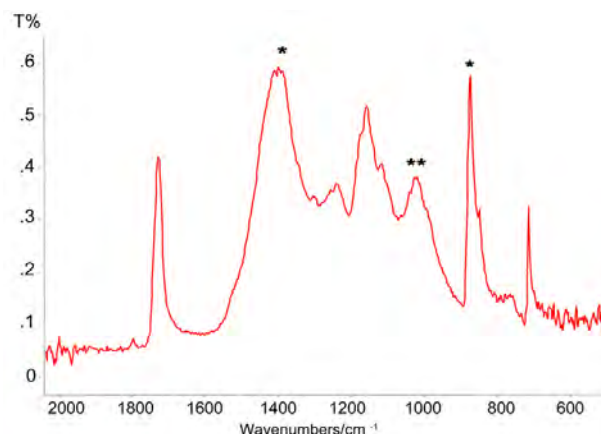


Figure 10: FTIR spectrum (ATR) of paint sample SF26, showing the specific IR bands of calcite (*) and ultramarine (**) along with the bands of the binder (EA/MMA).

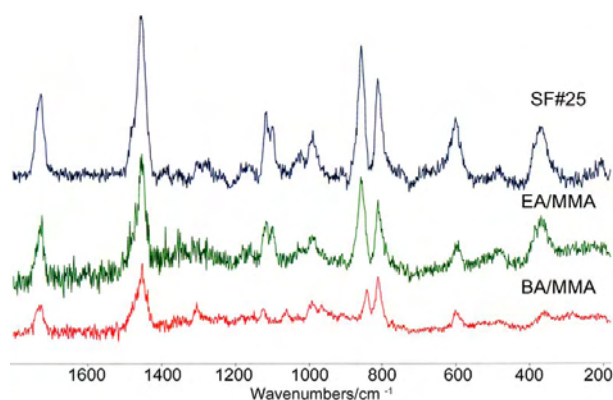


Figure 11: Raman spectra of paint sample SF25 and the two media EA/MMA and BA/MMA.

where, and show some noticeable differences, especially in the CH region³.

Elemental analysis of sample SF25 by SEM-EDX identified the presence of inorganic elements in the paint such as titanium (Ti), aluminum (Al), silicon (Si) and sulfur (S). Poorly crystallized silicates are indeed very weak Raman scatterers and their signal can therefore be overwhelmed by the strong scattering of the other components of the mixture (in this case, the binder). FTIR analyses did not detect the inorganic components either, probably because of their very low concentration. In both cases the absence of detection of the pigment would have led to a misinterpretation of the composition of the paint if additional analytical techniques had not been used.

3.3 Case Study: Untitled 1978

To complement the analyses carried out on the pre-mixed paints from his studio, eight micro-samples from one of Sam Francis' paintings *Untitled* (SFP78-18, 1978, Figure 12), an acrylic paint on canvas, were analyzed by FTIR and Raman microscopy (the samples were not embedded in

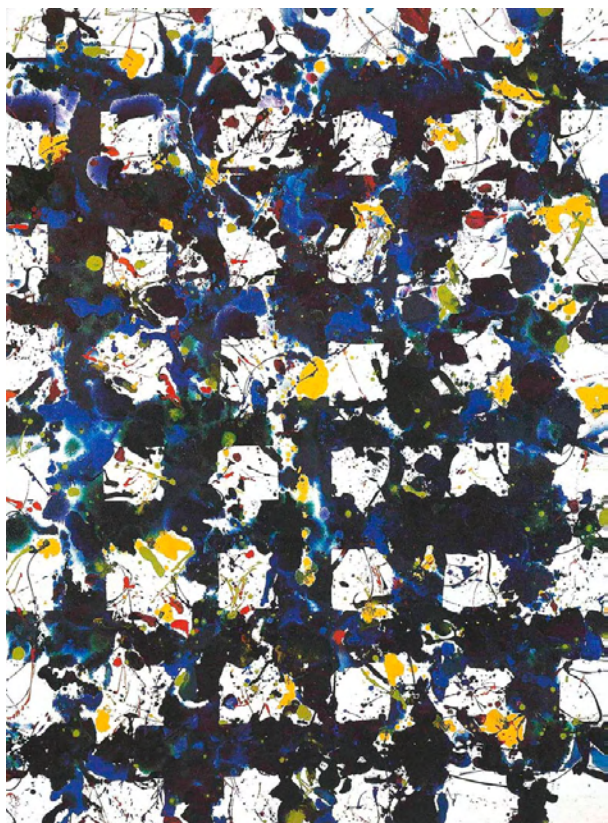


Figure 12: Untitled, 1978; 90"x60", Photo courtesy of Jonathan Novak Contemporary Art.

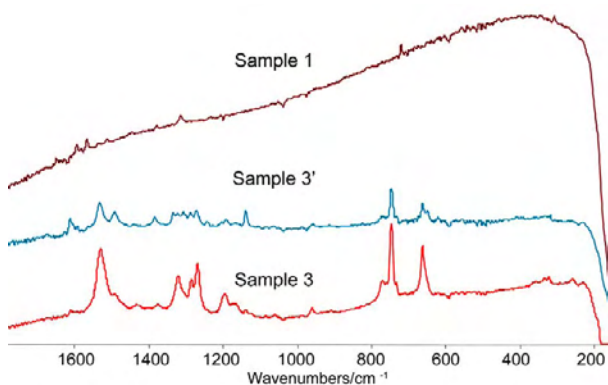


Figure 13: Raman spectra of samples #1 and #3 (2 different locations) from the painting Untitled.

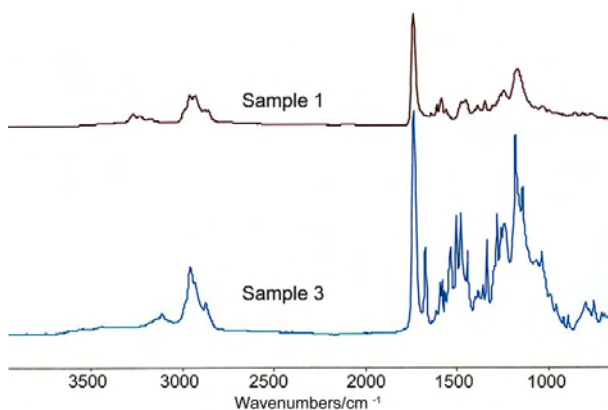


Figure 14: FTIR spectra (ATR) of sample #1 and sample #3 from the painting Untitled.

cross-sections to avoid any interference from the resin scattering during Raman analyses). The paint components were successfully identified and two samples (#1 and #3) especially demonstrated both the limitations of each technique, and their complementarity.

Figures 13 and 14 show the Raman and FTIR spectra of sample #1, taken from a dark-red coloured area in the left bottom edge. The Raman spectrum of this sample is dominated by very strong fluorescence that renders its precise characterization impossible, whereas the IR spectrum of the same micro-sample permits readily the identification of pigment PR122 (C.I. 73915, quinacridone) and a pEA/MMA medium.

The spectra obtained for sample #3, taken from a bright apple-green area on the left side of the painting, are also shown in Figures 13 and 14. Curiously while the Raman analyses indicated the presence of PG36 (C.I. 74265, chlorinated copper phthalocyanine), IR analyses pointed to PY3 (C.I. 11710, monoazo). The presence of both a yellow and a green pigment certainly made sense, from the yellowness and brightness of the green colour.

It was speculated that these apparently contradictory results might be a reflection of the relatively small size of the sample probed by Raman microscopy in comparison to FTIR. Therefore, further analyses were performed on multiple areas of the sample by Raman microscopy. Indeed, additional peaks appeared in one of the Raman spectra of the sample (Figure 13, sample #3), corresponding to the main and most intense Raman bands from PY3 (650, 747, 1141, 1243, 1311, 1337, 1385, 1496 and 1614 cm^{-1}) along with the most intense Raman bands of PG36 (662, 745, 772, 961, 1193, 1271, 1288, 1323 and 1535 cm^{-1}). PG 36, on the other hand, could not be detected with FTIR. This example serves to highlight the limitations of both techniques and the need to use multiple techniques in any investigation of complex mixture of unknown materials. Furthermore, it is demonstrated that FTIR and Raman spectroscopy are complementary rather than competing techniques.

4 Conclusion

The usefulness of Raman microscopy and infrared spectroscopy for the analyses of modern paints, with particular emphasis on the identification of synthetic organic pigments, was evaluated through the study of Sam Francis' materials and techniques. The study was carried out on a large set of pre-mixed, custom-made, paints found in his

Santa Monica studio, and in addition, one of his paintings was also sampled and analyzed.

Both Raman and FTIR spectroscopy provided valuable and in most cases detailed information. Raman microscopy generally gave better results for the pigments, both organic and inorganic. It offers higher resolution and the possibility for confocal measurements, but the risk of damaging the sample with the laser, and the autofluorescence of the sample may limit the applications of Raman microscopy in some cases. The accurate identification of the binding medium remains one of the important advantages of FTIR in the study of modern paints (in addition to its relatively low cost and availability to many museums and art research laboratories).

One major difficulty encountered with Raman microscopy was that a good reference database of modern organic and inorganic pigments does not yet exist, unlike FTIR where the IRUG database now contains several hundred of such spectra. In response to this, a wide range of reference Raman spectra of over 100 synthetic organic pigments was collected during this project to assist with the interpretation of data from the Francis paint samples, and these will now be made available to the IRUG database. It is clear that the centralization of easily accessible databases would vastly improve the processing of such analytical data, and it is hoped that other laboratories will submit their reference Raman spectra to the IRUG database.

5 Acknowledgements

The authors express their gratitude to Debra Burchett-Lere (Director of the Sam Francis Foundation), Aneta Zebala (Private Conservator), Albrecht Gumlich (GRI), Karen Trentelman and Herant Khanjian (both GCI).

6 References

1. C. Menke, R. Rivenc and T. Learner, *The use of direct temperature-resolved mass spectrometry (DTMS) in the analysis of acrylic paints used by Sam Francis*, Int. J. Mass. Spectrom., 2009, in press, doi:10.1016/j.ijms.2008.12.006
2. T. Learner, *The Use of a Diamond Cell for the FTIR Characterisation of Paints and Varnishes Available to Twentieth Century Artists*, Postprints: IRUG2 Meeting, 1998, 7-20.
3. T. Learner, *Analysis of modern paints*, Los Angeles: Getty Conservation Institute, 2004.
4. J. Jonsson, T. Learner, *Separation of Acrylic Paint Components and their Identification with FTIR Spectroscopy*, Postprints from the 6th Infrared and Raman Users Group Conference, 2004, 58-65.
5. S. Lomax, M. Schilling, T. Learner, *The identification of synthetic organic pigments by FTIR and DTMS*, in: T. Learner et al. Ed., *Modern Paints Uncovered*, Getty Conservation Institute, 2007, 105-117.
6. A. Rizzo, *Progress in the application of ATR-FTIR microscopy to the study of multi-layered cross-sections from works of art*, Anal. Bioanal. Chem., 2008, **392**, 47-55.
7. B. Guineau, *Non-destructive analysis of pigments by laser Raman microprobe spectrometry: examples of azurite and malachite*, Stud. Conserv., 1984, **29**, 35-41.
8. R. Davey, D.J. Gardiner, B.W. Singer, M. Spokes, *Examples of analysis of pigments from fine art objects by Raman microscopy*, J. Raman Spectrosc., 1994, **25**, 53-7.
9. D.C. Smith, M. Bouchard, M. Lorblanchet, *An initial Raman microscopic investigation of prehistoric rock art in caves of the Quercy District, S.W. France*, J. Raman Spectrosc., 1999, **30**, 347-354.
10. Ramos P.M., Ruisanchez I., *Data fusion and dual-domain classification analysis of pigments studied in works of art*, Anal. Chim. Acta, 2006, **558**, 274-282.
11. P. Vandenabeele, L. Moens, H.G.M. Edwards, R. Dams, *Raman spectroscopic database of azo pigments and application to modern art studies*, J. Raman Spectrosc., 2000, **31**, 509-517.
12. G.D. Smith, R.J.H. Clark, *Raman microscopy in art history and conservation science*, Rev. Conserv., 2001, **2**, 92-106.
13. I.R. Lewis, H.G.M. Edwards, eds, *Handbook of Raman Spectroscopy*, Practical Spectroscopy Series, Vol. 28, Marcel Dekker, New York, 2001.
14. L. Burgio, R.J.H. Clark, *Library of FT-Raman Spectra of Pigments, Minerals, Pigment Media and Varnishes, and Supplement to Existing Library of Raman Spectra of Pigments with Visible Excitation*, Spectrochim. Acta A, 2001, **57**, 1491-1521.
15. M. Bouchard, D.C. Smith, *A Catalogue of 45 Reference Raman Spectra of Minerals concerning research in Art History or Archaeology (corroded metals & stained glass)*, Spectrochim. Acta A, 2003, **59**, 2247-2266.
16. K. Castro, M. Perez-Alonso, M.D. Rodriguez-Laso, L.A. Fernandez, J.M. Madariaga, *On-line FT-Raman and dispersive Raman spectra database of artists' materials (e-VISART database)*, Anal. Bioanal. Chem., 2005, **382**, 248.
17. RASMIN - Raman Spectra Database of Minerals and Inorganic Materials (http://riodb.ibase.aist.go.jp/rasmin/E_index.htm, accessed 24/03/2009). © National Institute of Advanced Industrial Science and Technology (AIST).
18. R.T. Downs, *The RRUFF Project: an integrated study of the chemistry, crystallography, Raman and infrared spectroscopy of minerals*. Program and Abstracts of the 19th General Meeting of the International Mineralogical Association in Kobe, Japan. O03-13, 2006.
19. P. Ropret, S.A. Centeno, P. Bukovec, *Raman identification of yellow synthetic organic pigments in modern and contemporary paintings: Reference spectra and case studies*. Spectrochim. Acta A, 2008, **69A**, 486-497.
20. S. Lomax, T. Learner, *A Review of the classes, structures, and methods of analysis of synthetic organic pigments*, J. Am. Inst. Conserv., 2006, **45**, 107-125.
21. D. Lin-Vien, N.B. Colthup, W.G. Fateley, J.G. Grasselli, *The handbook of infrared and Raman characteristics frequencies of organic molecules*, Academic Press, San Diego, 1991.
22. P.J. Trotter, *Azo dye tautomeric structures determined by Laser-Raman spectroscopy*, Appl. Spectrosc., 1977, **31**, 30-35.
23. R.M. Silverstein, G.C. Bassler, T.C. Morrill, *Spectroscopic identification of organic compounds* (4th ed.). New York, Chichester, Brisbane, Toronto: John Wiley and Sons, 1981.

24. B. Ormsby, E. Kampsakali, C. Miliani, T. Learner, *A FTIR-based exploration of the effects of wet cleaning artists' acrylic emulsion paints*, e-Preserv. Sci., 2009, in print.
25. D.L.A. De Faria, S.V. Silva, M.T. De Oliveira, *Raman microspectroscopy of some iron oxides and oxyhydroxides*, J. Raman Spectrosc., 1997, **28**, 873-878.
26. D. Tranqui, A. Durif, J-C Guitel, M.T. Averbuch, *Bulletin de la Soc. De Mineralogie et de Cristallographie*, I, 1968, 10.
27. F. Kubel, *Crystal Structure of Lithium Cobalt Double Orthophosphate*, Z. Kristallogr., 1994, 290.
28. M. Bouchard, D.C. Smith, C. Carabatos-Nedelec, *An investigation of the feasibility of applying Raman microscopy for exploring stained glass*, Spectrochim. Acta A, 2007, **68A**, 1101-1113.
29. G. Burrafato, M. Calabrese, A. Cosentino, A.M. Gueli, S.O. Troja, A. Zuccarello, *ColoRaman project: Raman and fluorescence spectroscopy of oil, tempera and fresco paint pigments*, J. Raman Spectrosc., in press.
30. O.N. Shebanova, P. Lazor, *Raman spectroscopic study of magnetite (FeFe₂O₄): a new assignment for the vibrational spectrum*, J. Solid State Chem., 2003, **174**, 424-430.
31. Y. Wang, D.C. Alsmeyer, R.L. McCreery, *Raman spectroscopy of carbon materials: structural basis of observed spectra*, Chem. Mat., 1990, **2**, 557-63.
32. F. Buciuman, F. Patcas, R. Craciun, D.R.T. Zahn, *Vibrational spectroscopy of bulk and supported manganese oxides*, Phys. Chem. Chem. Phys., 1999, **1**, 185-190.
33. J. Ferraro, *The Sadtler infrared spectra handbook of minerals and clays*, Heyden Ed. 1982, 440.
34. J.A. Gadsden, *Infrared spectra of minerals and related inorganic compounds*, Butterworths, London, 1975.
35. B. Plav, S. Kobe, B. Orel, *Identification of crystallization forms of CaCO₃ with FTIR spectroscopy*, Kovine Zlitrine Tehnol., 1999, **33**, 6.
36. V. Desnica, K. Furic, M. Schreiner, *Multianalytical Characterization of a variety of Ultramarine pigments*, e-Preserv. Sci., 2004, **1**, 15-21.